Generation of Flat-Top Q-Switched Envelope Dissipative Soliton Resonance Pulse in Passively Mode-Locked Fiber Laser
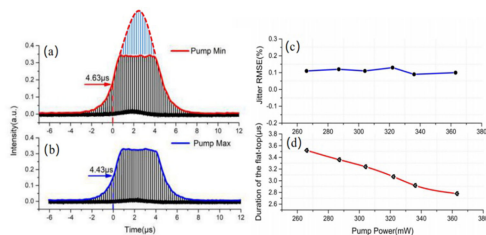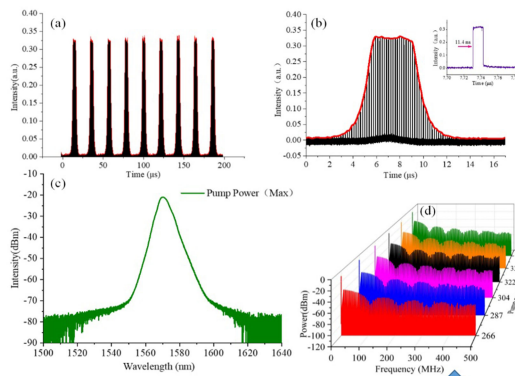
Long Han
Tianshu Wang
Runmin Liu
Wanzhuo Ma
Yiwu Zhao
Qiang Fu
Huilin Jiang

Schematic configuration of flat-top Q-switched mode-locked (FT-QML) dissipative soliton resonance pulse fiber laser

(a-b) the flat-top envelope at minimum pump power and maximum power (c) Amplitude jitter in the flat-top period (d) Duration of the flat-top envelope

(a) The FT-QML DSR envelopes (b) Details of single FT-QML DSR envelope. Inset: Single mode-locked pulse (c) optical spectrum at maximum power (d) Corresponding RF spectrum
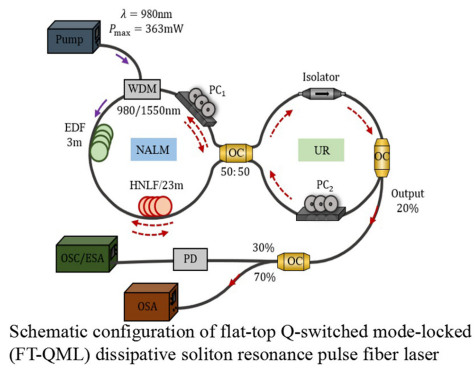
IEEE

Generation of Flat-Top Q-Switched Envelope Dissipative Soliton Resonance Pulse in Passively Mode-Locked Fiber Laser

Long Han,[1,2] **Tianshu Wang** [1,2] **Runmin Liu,**[1,2] **Wanzhuo Ma,**[1,2] **Yiwu Zhao,**[1,2] **Qiang Fu,**[1,2] **and Huilin Jiang**[1,2]

[1]National and Local Joint Engineering Research Center of Space Opto-electronics Technology, Changchun University of Science and Technology, Changchun 130022, China
[2]College of Opto-Electronic Engineering, Changchun University of Science and Technology, Changchun 130022, China

Abstract: We present demonstration of an erbium-doped fiber laser based on the nonlinear amplifying loop mirror mechanism, with a stable phenomenon of flat-top Q-switched mode-locked (FT-QML) dissipative soliton resonance (DSR) pulse, for the first time. In the experiment, we can observe both the flat-top Q-switched envelope and square-wave pulse by the peak power clamping effect inside the cavity. The characteristics of both continuous DSR pulse and flat-top Q-switched mode-locked square-wave are analyzed comprehensively. With the maximum pump power of 363 mW, single pulse energy in the FT-QML envelope can be up to 14 nJ as three times high as the one of continuous DSR. Essentially, the temporal width of the Q-switched mode-locked envelope can reach 4.6 μs with flat-top duration of 3.5 μs. The amplitude fluctuation of the sub-pulse inside the flat-top is stable at about 0.12% by using the formula of RMSE. Therefore, the laser can provide flat-top burst mode pulse sequence, and the pulse width can be controlled by tuning the pump power.

Index Terms: Dissipative soliton resonance, Q-switched envelope, mode-locked.

1. Introduction

In recent years, passively mode-locked fiber lasers have become one of the research hotspots amongst researchers around the world due to the significant advantages of their compact structure and easy integration, fine stability, high energy conversion efficiency. Moreover, it can output the high peak power and ultra-short pulses. Therefore, passively mode-locked fiber lasers have great development prospects in the fields of laser communication, material processing and medical surgery. The main methods for implementing passively mode-locked fiber lasers are semiconductor saturated absorber (SESAM), nonlinear amplifying loop mirror (NALM), nonlinear optical loop mirror (NOLM) and nonlinear polarization rotation (NPR) technology [1]–[4]. Generally, the mode-locked fiber laser resonator can be composed of optical fibers with different dispersion parameters. Due to the different distribution and arrangement of dispersion in the cavity, the mode-locked fiber laser can output traditional soliton, dispersion management soliton and dissipative soliton [5]–[7].

However, these types of solitons have the same feature that as the effect of the overdriven nonlinearity, namely that it can cause the generation of wave-breaking with increasing the energy of mode-locked pulse [8]. The energy of these types of solitons can be limited by the saturation energy of the mode-locked mechanism [9].

As a higher energy pulse, dissipative soliton resonance (DSR) was theoretically proposed by Chang *et al.* in anomalous dispersion regime for the first time [10]. Generally, the pulse temporal width can tune from picoseconds to nanoseconds or even longer. It can be observed experimentally in net positive dispersion and net negative dispersion regions [11]–[14]. One of the most remarkable features of the DSR phenomenon is that the pulse width and the pulse energy can increase linearly with the enhancing of the pump power. The processing of increment of the pulse width and energy cannot cause the pulse wave-breaking as well as the amplitude remains substantially unchanged. However, the research focus of the dissipative soliton resonance is mainly concentrated on how to further improve and enhance the output pulse energy, pulse duration and amplitude adjustment of the laser. In 2015, Krzempek *et al.* reported an all-fiber erbium-ytterbium co-doped double-clad fiber laser based on NALM, the pulse energy output directly from the cavity was 2.13 μJ without a Q-switched operation or an additional amplifier [15]. Then, the DSR pulse was experimentally studied in a passively mode-locked eight-cavity fiber laser, and square-wave pulse with pulse width from 135 to 2272 ns with no wave-breaking can be found [16]. In 2016, Georges Semaan showed a passively mode-locked eight-cavity fiber laser with two amplifiers [17], and the amplitude and width of the output beam can be controlled independently by adjusting the power of each amplifier. In 2017, Deng *et al.* used a nonlinear polarization rotation technique combined with a saturated carbon nanotube absorber to switchable generate a rectangular noise-like pulse and a dissipative soliton resonance using 65-meter highly nonlinear fibers, for the first time [18].

Generally, with the gradual increasing of the pump power or variation of nonlinear characteristics in the cavity, the fiber laser can operate separately in the Q-switched state, the continuous wave mode-locked and Q-switched mode-locked (QML) state. The Q-switched mode-locked has the characteristics of Q-switched operation and mode-locked state simultaneously. Essentially, Q-switched mode-locked can produce higher pulse energy in the case of the same output average power [19]. To date, passively Q-switched mode-locked operation has been achieved primarily with the aid of saturable absorbers, such as semiconductor saturable absorber mirrors (SESAMs) [20], carbon nanotubes [21], graphene [22], and MoS_2 [23]. However, additional optical components can be required in the cavity, which can result in greater insertion loss and make the system more cumbersome. In addition, the current technology for manufacturing graphene and carbon nanotubes is still relatively complicated. In recent years, the nonlinear polarization evolution (NPE) and NALM technique as artificial saturable absorber effect are also suitable for the generating of Q-switched pulse in fiber lasers [24]–[26]. It is worth mentioning that a type of peak-power-clamping (PPC) effect in passive Q-switched regime can be achieved in the NPR thulium/holmium co-doped fiber laser by intracavity-incorporating a segment of highly nonlinear fiber (HNLF) and launching high-enough pump power in Ref. [25]. This work has a greater benefit for the deeper understanding of the formation of the Q-switched operation. Furthermore, the average single pulse energy of the 1.9 μm Q-switched mode-locked square-wave fiber laser is three times more than that of continuous dissipative soliton resonance was reported [26]. Nevertheless, it is rarely reported about the technique of combining passively Q-switched mode-locked and the generation of dissipative soliton resonance in the 1.55 μm band.

In this paper, we demonstrate experimentally a type flat-top Q-switched mode-locked dissipative soliton resonance pulse based on the erbium-doped passively mode-locked figure-eight cavity. With the pump power increasing from 266 to 363 mW, the pulse duration of continuous DSR can be broadened from 2 to 2.85 ns, and the corresponding maximum single pulse energy is as large as 5 nJ. With the enhancement of pump power, the repetition rate of flat-top Q-switched envelope can change from 38.6 to 47 kHz, and the maximum energy of single envelope is 420 nJ. What's more, at the maximum pump power of 363 mW, single pulse energy in the FT-QML envelope is 14 nJ equivalent to 2.8 times high the energy of the continuous DSR. The duration of the flat-top envelope varies from 2.8 to 3.5 μs within the tuning range of pump power. The pulse amplitude
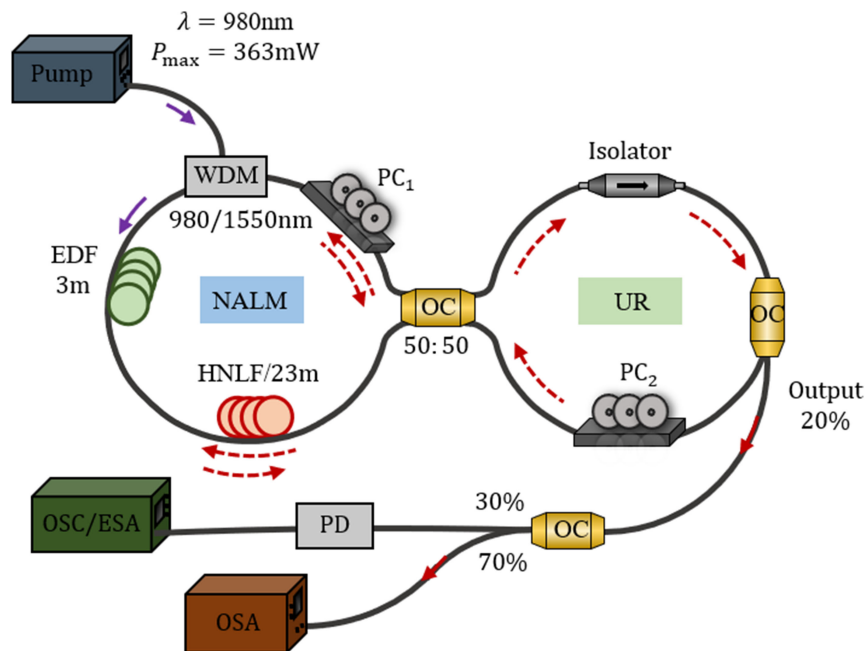
Fig. 1. Schematic configuration of flat-top Q-switched mode-locked dissipative soliton resonance pulse fiber laser. EDF: Erbium-doped fiber, WDM: Wavelength division multiplexer, HNLF: Highly nonlinear fiber, PC1 versus PC2: Polarization controllers, ISO: Polarization insensitive isolator, and OC: Optical coupler.

jitter in the flat-top temporal domain is stable at around 0.12%. The work can open new ways of achieving the flat-top burst mode pulse sequence.

2. Experimental Setup

The experimental configuration is schematically shown in Fig. 1. A figure-eight resonator including a NALM and a unidirectional loop. The left loop is built in a standard NALM configuration. A segment of 3 m single-mode erbium-doped fiber with doping concentration of 4.5 dB/m and group velocity dispersion (GVD) parameter of about 31 ps^2/km is used as the gain fiber. A 980 nm laser diode pump with maximum pump power of 363 mW is coupled into the fiber laser resonator via a wavelength division multiplexer (WDM). The imbalance in accumulated phase shift for two opposite directions propagating pulses can be achieved by participating an additional a segment of 23 m-long highly nonlinear fiber (HNLF, NL-1550-POS) with nonlinear coefficient of 10/W/km and dispersion coefficient of 3 ps/nm/km at 1550 nm. The HNLF has the high nonlinearity and low dispersion slope simultaneously. The right loop including a polarization-independent isolator (PI-ISO) and a polarization controller (PC) can connect the NALM by a 50/50 optical coupler (OC). The laser output is extracted from the ring cavity by 80:20 fiber coupler, and the 20% port can be used to output. The total length of the laser is 39 m corresponding to the fundamental repetition rate of 5.3 MHz. The net GVD can be calculated -0.29 ps^2, thus the laser operates in the negative dispersion region.

The output optical spectrum can be monitored by an optical spectrum analyzer (OSA, YOKO-GAWA AQ6370D) through the 50% port of the external OC with the resolution of 0.05 nm. The output pulses can be detected by a 1.55 μm photo detector (PD) with 10 GHz bandwidth. An oscilloscope (Agilent DSO925A) with the bandwidth of 2.5 GHz and a radio frequency spectrum analyzer (FSA, Agilent, N9030A) with the frequency range from 3 Hz to 44 GHz are used to study the output pulse sequence in the time and frequency domain, respectively.
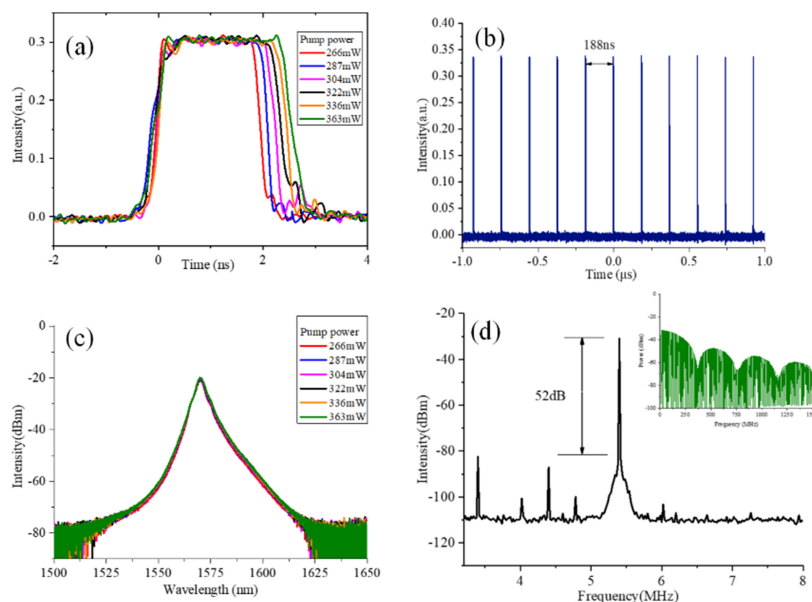
Fig. 2. The evolution of continuous DSR pulses. (a) Single pulse variation. (b) Pulse train. (c) Optical spectrum. (d) Fundamental frequency RF spectrum Inset: RF spectrum with 1.5GHz scanning.

3. Experimental Results and Discussions

In the experiment, the laser can realize the self-starting of the mode-locked when the pump power is up to 160 mW. By slightly adjusting the pump power and the parameters of the resonant cavity, multiple operating states can be observed, such as soliton rains and soliton clusters. By increasing the pump power to 180 mW and adjusting PC1 and PC2 repeatedly, and the dissipative soliton resonance pulse can be obtained. In order to lucubrate the characteristics of DSR pulses, first of all, the position of the PCs is fixed. The amplitude of the pulse remains constant, while the pulse duration is increased from 2 to 2.85 ns, as shown in Fig. 2(a). Fig. 2(b) depicts the pulse sequence of the mode-locked laser. The pulse interval is 188ns corresponding to the cavity round-trip time. The pulse spectrum curves produced by different pump power is shown in Fig. 2(c). With the center at 1570 nm with 3-dB spectral bandwidth of 3.6 nm, the triangle-shape spectrum is a typical feature of DSR pulse. The fundamental frequency of the mode-locked pulse is 5.3 MHz depending on the cavity length. The signal-to-noise ratio (SNR) is 52 dB as shown in Fig. 2(d). At the maximum pump power of 363 mW, the evolution of the RF spectrum can be shown in illustration of Fig. 2(d). The spectrum analyzer can be adjusted to 1.5 GHz with a resolution bandwidth of 1kHz. As the pump power increases from 266 to 363 mW, the periodic frequency of the characteristic modulation can decrease from 478 to 350 MHz corresponding to the pulse width from 2 to 2.85 ns. The modulation frequency is theoretically equal to the reciprocal of the single pulse width.

In the experiment, the intra-cavity birefringence effect and the loss are changed by rising the pump power to 210 mW, and the Q-switched mode-locked operation can be obtained properly adjusting a pair of three-ring polarization controllers. In the cavity, a longer recovery time of saturation absorption is needed, when continuous wave mode-locked operation evolves into the Q-switched mode-locked operation. Fig. 3(a) shows the envelope train within the scanning range of 200 μs, and the curve fitting of the Q-switched envelope can be achieved by utilizing the Eq. (1) of the Ref. [26]. The envelope interval is 21.2 μs. Enlarged graphics of a singly Q-switched pulse envelop is shown in Fig. 3(b) at the maximum pump power of 363 mW. Through the fitting of the envelope, it can be seen that the pulse duration of single Q-switched envelope is 4.43 μs. The inset of Fig. 3(b) shows the details of a pulse waveform inside envelope, and a square-wave shape with the pulse width of 11ns can be clearly observed. At the maximum pump power, the
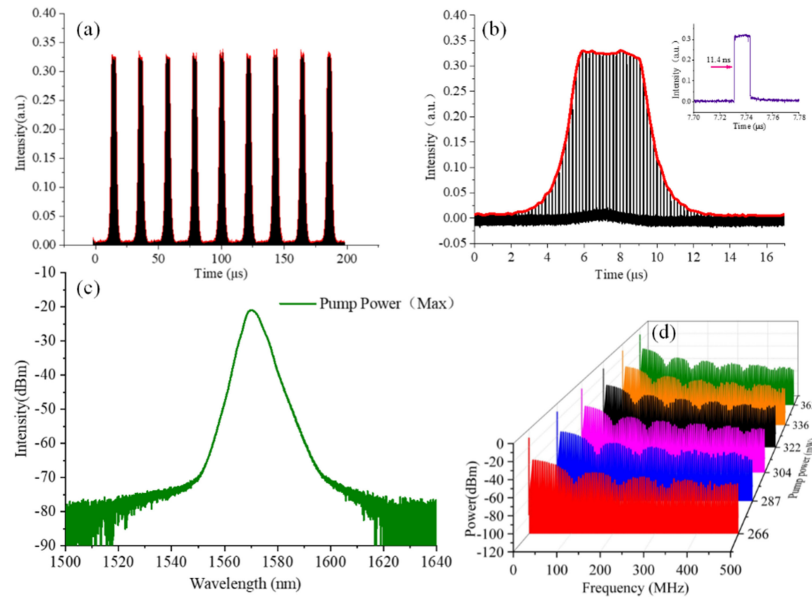
Fig. 3. The evolution of Q-switched mode-locked DSR operation. (a) Oscilloscope trace of Q-switched mode-locked DSR envelopes with 200μs scanning. (b) Details of single Q-switched mode-locked DSR envelope. Solid red line: fitting curve of single envelope Inset: Single mode-locked pulse. (c) optical spectrum at maximum power. (d) Corresponding RF spectrum with increasing pump power.
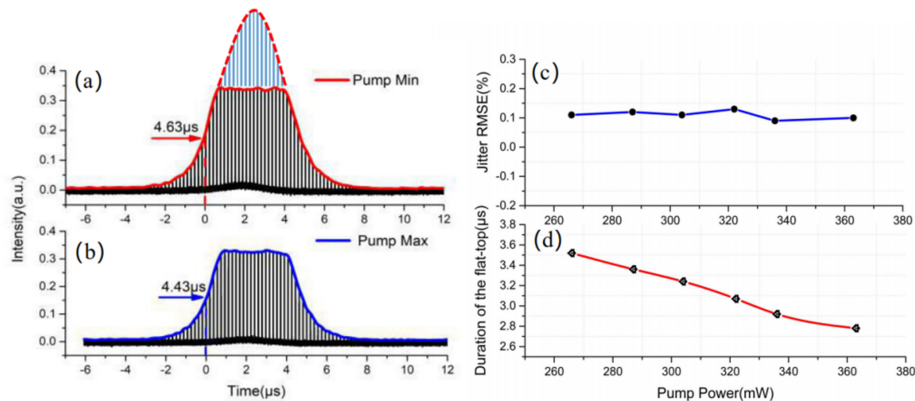

Fig. 4. The evolution of FT-QML envelope. (a) The flat-top envelope at minimum pump power. Red dashed line and solid line as a whole: the fit curve of the conventional Q-switched envelope. (b) The flat-top envelope at maximum pump power. (c) Amplitude jitter in the flat-top period with the rising of pump power. (d) Duration of the flat-top with the rising of pump power.

spectrum of the QML square-wave pulse is shown in Fig. 3(c). The spectrum has the center wavelength of 1570 nm and a 3 dB bandwidth of 5.6 nm which is slightly higher compared with that of continuous DSR. The RF trace evolution is presented with the pump-power-related, as shown in Fig. 3(d). The modulation period of the envelope can reduce from 107.1 to 87.3 kHz corresponding to the changing of single pulse duration from 9.3 to 11.4 ns. The spectrum scanning range and resolution bandwidth are 500 MHz and 1 kHz, respectively.

In the experiment, it comes to our attention that a flat-top phenomenon can be appeared in the envelope of Q-switched mode-locked operation called flat-top Q-switched mode-locked (FT-QML). In previously reported literatures [27–29], the shape of the parabola can be presented by the curve fitting of the single envelope as shown in Fig. 4(a) with consisting of solid red and dashed lines.
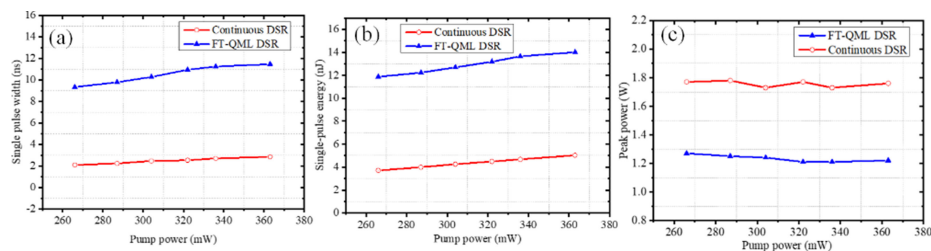
Fig. 5. Comparison of output parameters of continuous DSR pulse versus the FT-QML DSR pulse. (a) Single pulse width as a function of pump power. (b) Single pulse energy as a function of pump power. (c) Average peak power as a function of pump power.

The duration of the single envelope varies from 4.63 to 4.43 μs with the pump power rising from 266 to 363 mW as shown in Fig. 4(a) and Fig. 4(b). The maximum single envelope width is up to 1.5 times that of the reported in Ref. [26]. Specially, the longest pulse duration can reach as long as 3.5 μs when the pump power is fixed at 266 mW. In order to study the evolution of this particular phenomenon, the percentage of amplitude jitter inside the flat-top envelope and the flat-top width of single envelope are recorded separately under different pump powers as shown in Fig. 4(c) and Fig. 4(d). The former can be estimated using the expression of root-mean-square error (RMSE):

$$RMSE = \sqrt{\frac{\sum_{i=1}^{N} (X_i - X_{mean})^2}{N}} \qquad (1)$$

Where N is the number of sub-pulses in flat-top envelope, X_i is each pulse amplitude value in the flat-top period, X_{mean} is average amplitude value of the pulses. The percentages of amplitude jitter can be basically maintained at around 0.12% which show the perfect uniformity. Thus, it indicates that the flat-top operation is in a highly stable condition. The duration of the flat-top envelope can almost decrease linearly from 3.5 to 2.8 μs when the pump power increases from 266 to 363 mW as shown in Fig. 4(d). It can be suggested that the duration of the flat-top envelope can be controlled by changing the pump power.

In Ref. [25], the peak-power-clamping Q-switched (PPC-QS) operation with NPR technique has been reported firstly, and the pulse peak power can stay at a constant level as the rising of the pump power. The repetition rate of FT-QML varying continuously with pump power implies that the FT-QML has a typical feature of all Q-switched operation. Compared to PPC-QS phenomenon, the peak power clamping effect is even more pronounced in the experiment due to a longer highly nonlinear fiber which accumulates more nonlinear effect in the cavity. In addition, the PPC-QS phenomenon shows a passively Q-switched operation exclusively without generating of the square-wave mode-locked pulses. The pulse width (4.6 μs) in the single envelop of FT-QM at the maximum pump power of 363 mW which is over four times than that of PPC-QS (904.1 ns) at the pump power of 1.8 W. Furthermore, it can be noted that the phenomenon of FT-QML is not observed in our previous report [26]. It is estimated that there are no highly nonlinear fibers added to the ring cavity.

Similar to the PPC-QS phenomenon, the envelope of the FT-QML operation is affected by the peak power clamping effect. As a result, the sub-pulses in the central part of the envelope are suppressed. We further emphasis that the DSR pulses can be generated in the experiment, that is to say, the peak power can reach the saturation gain point when the gain and loss reach balance in the cavity. At this point, the peak power of the pulse is clamped in a region of maximum transmission of the loop [30]–[31]. Based on the above analyses, we can conclude that both the flat-top envelope and formation of DSR pulse can be caused by the dual influence of the PPC effect. The width of the sub-pulses in the envelope is broadened obviously with the pump strength compared with continuous DSR pulse as shown in Fig. 5(a). For instance, with the pump power of 363 mW, the single pulse width of the continuous DSR and the FT-QML are up to 2.85 ns and 11.4 ns, respectively. In addition, the modulation frequency of Q-switched envelope and the duration of the

flat-top clamp can be controlled by turning the pump power. Simultaneously, the sub-pulses in the FT-QML envelope have well uniformity of amplitude, therefore, the laser can be utilized as the conducive way to generate the flat-top burst mode pulse train which is playing a crucial role in the material processing or species measurements and laser ablation of materials [32]–[34].

In terms of a research of the pulse characteristics of continuous DSR and FT-QML square-wave, we record several key characteristic parameters of the output pulse including pulse duration, pulse energy, repetition rate and peak power. The maximum single envelope energy of FT-QML is 420 nJ corresponding to the modulation frequency of 44 kHz. Single pulse width of FT-QML square-wave pulse can change from 9.3 to 11.4 ns which is four times than that of continuous DSR pulse. Single pulse energy in the envelope of FT-QML operation can be expressed as,

$$E_Q = \frac{P_0}{NR} \tag{2}$$

P_0 is average output power, N is the number of pulses in the Q-switched envelope, R is the repetition rate of the Q-switched envelope. As the pump power increases, the average single pulse energy can increase from 11.8 to 14 nJ, as shown in Fig. 5(b). According to formula in Ref. [27], single pulse peak power of FT-QML operation is,

$$P_f = \frac{P_0}{NRT_0} \tag{3}$$

T_0 is the pulse width of the mode-locked pulses. As the number of pulses in the single Q-switched envelope can reduce from 35 to 30, the peak power can be above 1.2 W when the peak power of continuous DSR is stable about 1.7 W as shown in Fig. 5(c). Single pulse width of FT-QML is increased obviously, resulting in reduced the peak power. It is important to emphasize that the slope of the blue curve is higher than that of the red curve in Fig. 5(a). The flat-top Q-switched mode-locked DSR pulse is formed by two different mechanisms, the NALM mechanism and Q-switched mechanism. The flat-top Q-switched mode-locked DSR pulses are dually affected by the peak power clamping effect. The high nonlinear fibers is used in the configuration, which makes more nonlinear effects accumulate in the resonant cavity. Therefore, the normal Q-switched envelope pulse is affected by the peak power clamping effect, and the top of the Q-switched envelope tends to be flat. Of course, the amplitude of sub-pulses in the flat-top Q-switched envelope also decline, as shown in Fig. 5(c).

4. Conclusion

In conclusion, we demonstrate and implement the continuous dissipative soliton resonance and the flat-top Q-switched mode-locked square-wave pulse based on the NALM technique. The single pulse energy of continuous DSR can reach up to 5 nJ with the fundamental repetition rate of 5.3 MHz. By changing the pump power and the resonator parameters, the flat-top Q-switched mode-locked phenomenon can be observed. The sufficient length highly nonlinear fiber in the cavity can play the essential role of the generation of flat-top Q-switched mode-locked operation. At the maximum pump power of 363 mW, the energy of single Q-switched envelope is 420 nJ, and the single pulse duration in the Q-switched envelope is 11.4 ns, simultaneously, the single pulse energy is up to 14 nJ. The amplitude jitter of the sub-pulses inside the flat-top time domain is basically keeping consistency at 0.12%. The laser can output the flat-top burst mode pulse sequence with the variable pulse width. This research can open new avenues for exploration of formation of both dissipative soliton pulses and the Q-switched mode-locked mechanism.

References

[1] H. Zhang, Q. L. Bao, D. Y. Tang, L. M. Zhao, and K. P. Loh, "Large energy soliton erbium-doped fiber laser with a graphene-polymer composite mode locker," *Appl. Phys. Lett.*, vol. 95, no. 14, 2009, Art. no. 141103.

[2] M. E. Fermann, F. Haberl, M. Hofer, and H. Hochreiter, "Nonlinear amplifying loop mirror," *Opt. Lett.*, vol. 15, no. 13, pp. 752–754, 1990.

[3] X. Feng, H. Y. Tam, and P. K. A. Wai, "Stable and uniform multiwavelength erbium-doped fiber laser using nonlinear polarization rotation," *Opt. Express*, vol. 14, no. 18, pp. 8205–8210, 2006.

[4] Z. X. Zhang, K. Xu, J. Wu, X. B. Hong, and J. T. Lin, "Multiwavelength figure-of-eight fiber laser with a nonlinear optical loop mirror," *Laser Phys. Lett.*, vol. 5, no. 3, pp. 213–216, 2008.

[5] J. D. Kafka, T. Baer, and D. W. Hall, "Mode-locked erbium-doped fiber laser with soliton pulse shaping," *Opt. Lett.*, vol. 14, no. 22, pp. 1269–1271, 1989.

[6] K. Tamura, E. P. Ippen, H. A. Haus, and L. E. Nelson, "77-fs pulse generation from a stretched-pulse mode-locked all-fiber ring laser," *Opt. Lett.*, vol. 18, no. 13, pp. 1080–1082, 1993.

[7] A. Cabasse, B. Ortaç, G. Martel, A. Hideur, and J. Limpert, "Dissipative solitons in a passively mode-locked Er-doped fiber with strong normal dispersion," *Opt. Express*, vol. 16, no. 23, pp. 19322–19329, 2008.

[8] D. Anderson, M. Desaix, M. Lisak, and M. L. Quiroga–Teixeiro, "Wave breaking in nonlinear-optical fibers," *J. Opt. Soc. Am B*, vol. 9, no. 8, pp. 1358–1361, 1992.

[9] D. Y. Tang, L. M. Zhao, B. Zhao, and A. Q. Liu, "Mechanism of multisoliton formation and soliton energy quantization in passively mode-locked fiber lasers," *Phys. Rev. A*, vol. 72, no. 4, 2005, Art. no. 043816.

[10] W. Chang, A. Ankiewicz, J. M. Soto-Crespo, and N. Akhmediev, "Dissipative soliton resonances," *Phys. Rev. A*, vol. 78, no. 2, 2008, Art. no. 023830.

[11] X. Wu, D. Y. Tang, H. Zhang, and L. M. Zhao, "Dissipative soliton resonance in an all-normal-dispersion erbium-doped fiber laser," *Opt. Express*, vol. 17, no. 7, pp. 5580–5584, 2009.

[12] L. Duan, X. Liu, D. Mao, L. Wang, and G. Wang, "Experimental observation of dissipative soliton resonance in an anomalous-dispersion fiber laser," *Opt. Express*, vol. 20, no. 1, pp. 265–270, 2012.

[13] S. K. Wang, Q. Y. Ning, A. P. Luo, Z. B. Lin, Z. C. Luo, and W. C. Xu, "Dissipative soliton resonance in a passively mode-locked figure-eight fiber laser," *Opt. Express*, vol. 21, no. 2, pp. 2402–2407, 2013.

[14] Z. C. Luo, W. J. Cao, Z. B. Lin, Z. R. Cai, A. P. Luo, and W. C. Xu, "Pulse dynamics of dissipative soliton resonance with large duration-tuning range in a fiber ring laser," *Opt. Lett.*, vol. 37, no. 22, pp. 4777–4779, 2012.

[15] K. Krzempek, "Dissipative soliton resonances in all-fiber Er-Yb double clad figure-8 laser," *Opt. Express*, vol. 23, no. 24, pp. 30651–30656, 2015.

[16] T. Liu, D. Jia, Y. Liu, Z. Wang, and T. Yang, "Generation of microseconds-duration square pulses in a passively mode-locked fiber laser," *Opt. Commun.*, vol. 356, pp. 416–420, 2015.

[17] G. Semaan, F. B. Braham, J. Fourmont, M. Salhi, F. Bahloul, and F. Sanchez, "10 μJ dissipative soliton resonance square pulse in a dual amplifier figure-of-eight double-clad Er: Yb mode-locked fiber laser," *Opt. Lett.*, vol. 41, no. 20, pp. 4767–4770, 2016.

[18] Z. S. Deng *et al.*, "Switchable generation of rectangular noise-like pulse and dissipative soliton resonance in a fiber laser," *Opt. Lett.*, vol. 42, no. 21, pp. 4517–4520, 2017

[19] C. Hönninger, R. Paschotta, F. Morier-Genoud, M. Moser, and U. Keller, "Q-switching stability limits of continuous-wave passive mode locking," *J. Opt. Soc. Am B*, vol. 16, no. 1, pp. 46–56, 1999.

[20] J. F. Li, D. D. Hudson, Y. Liu, and S. D. Jackson, "Efficient 2.87 μm fiber laser passively switched using a semiconductor saturable absorber mirror," *Opt. Lett.*, vol. 37, no. 18, pp. 3747–3749, 2012.

[21] J. Liu, Y. Q. Li, L. H. Zheng, L. B. Su, J. Xu, and Y. G. Wang, "Passive Q-switched mode locking of a diode-pumped Tm:SSO laser near 2 μm," *Laser Phys. Lett.*, vol. 10, 2013, Art. no. 105812.

[22] C. Feng, D. Liu, and J. Liu, "Graphene oxide saturable absorber on golden reflective film for Tm: YAP Q-switched mode-locking laser at 2 μm," *J. Modern Opt.*, vol. 59, no. 21, pp. 1825–1828, 2012.

[23] L. C. Kong *et al.*, "Passive Q-switching and Q-switched mode-locking operations of 2 μm Tm: CLNGG laser with MoS$_2$ saturable absorber mirror," *Photon. Res.*, vol. 3, no. 2, pp. A47–A50, 2015.

[24] X. He *et al.*, "A stable 2 μm passively Q-switched fiber laser based on nonlinear polarization evolution," *Laser Phys.*, vol. 24, no. 8, 2014, Art. no. 085102.

[25] J. Zhao, L. Li, L. Zhao, D. Tang, and D. Shen, "Peak-power-clamped passive q-switching of a thulium/holmium Co-doped fiber laser," *J. Lightw. Technol.*, vol. 36, no. 20, pp. 4975–4980, Oct. 15, 2018.

[26] W. Z. Ma *et al.*, "1.9 μm square-wave passively Q-witched mode-locked fiber laser," *Opt. Express*, vol. 26, no. 10, pp. 12514–12521, 2018.

[27] J. H. Lin, H. R. Chen, H. H. Hsu, M. D. Wei, K. H. Lin, and W. F. Hsieh, "Stable Q-switched mode-locked Nd3+: LuVO4 laser by Cr4+: YAG crystal," *Opt. Express*, vol. 16, no. 21, pp. 16538–16545, 2008.

[28] Z. Wang *et al.*, "Multilayer graphene for Q-switched mode-locking operation in an erbium-doped fiber laser," *Opt. Commun.*, vol. 300, no. 15, pp. 17–21, 2013.

[29] Y. M. Chang, J. S. Li, and J. H. Li, "A Q-switched, mode-locked fiber laser employing subharmonic cavity modulation," *Opt. Express*, vol. 19, no. 27, pp. 26627–26633, 2011.

[30] L. Mei *et al.*, "Width and amplitude tunable square-wave pulse in dual-pump passively mode-locked fiber laser," *Opt. Lett.*, vol. 39, no. 11, pp. 3235–3237, 2014.

[31] G. Semaan, F. B. Braham, J. Fourmont, M. Salhi, F. Bahloul, and F. Sanchez, "10 μJ dissipative soliton resonance square pulse in a dual amplifier figure-of-eight double-clad Er: Yb mode-locked fiber laser," *Opt. Lett.*, vol. 41, no. 20, pp. 4767–4770, 2016.

[32] N. B. Jiang, M. C. Webster, and W. R. Lempert, "Advances in generation of high-repetition-rate burst mode laser output," *Appl. Opt.*, vol. 48, no. 4, pp. B23–B31, 2009.

[33] M. E. Smyser, K. A. Rahman, M. N. Slipchenko, S. Roy, and T. R. Meyer, "burst-mode Nd: YAG laser for kHz–MHz bandwidth velocity and species measurements," *Opt. Lett.*, vol. 43, no. 4, pp. 735–738, 2018.

[34] M. Lapczyna, K. P. Chen, P. R. Herman, H. W. Tan, and R. S. Marjoribanks, "Ultra high repetition rate (133 MHz) laser ablation of aluminum with 1.2-ps pulses," *Appl. Phys. A*, vol. 69, no. 1, pp. S883–S886, 1999.